JOURNAL OF CATALYSIS **159,** 340–352 (1996)
ARTICLE NO. 0096

Transmission Electron Microscopy and Energy Dispersive X-Ray Spectroscopy Studies of Pt–Sn/γ-Al_2O_3 Catalysts

Z. Huang, J. R. Fryer, C. Park, D. Stirling,[1] and G. Webb

Department of Chemistry, University of Glasgow, Glasgow G12 8QQ, United Kingdom

Received March 1, 1995; revised June 13, 1995

A series of Pt–Sn/γ-Al_2O_3 reforming catalysts have been prepared and studied by transmission electron microscopy (TEM) and energy-dispersive X-ray spectroscopy (EDX). It has been shown that the catalyst performance is dependent on the way in which the catalyst had been prepared. The majority of the tin was in the ionic state as Sn(II) while a minor part of the tin was reduced to the metallic state by platinum. Pt–Sn alloys were found together with platinum particles in the bimetallic catalysts. A significant number of very small TEM-invisible platinum particles less than 1 nm in diameter were present in addition the TEM-visible platinum particles. Particle aggregation and alloy formation occurred during the use of the catalysts in the reforming of octane. © 1996 Academic Press, Inc.

INTRODUCTION

The addition of tin to Pt/γ-Al_2O_3 improves both the selectivity to aromatics and the stability of the catalyst in catalytic reforming reactions. Extensive studies have been made in order to understand the origin of the beneficial effects of the tin in the bimetallic catalyst. The main points of contention have included the distribution and the chemical state of tin; the interaction between tin, platinum, and the support; the most notably, the tendency for platinum and tin to form alloys. The role of alloy formation in the improvement of catalyst performance has been of particular interest. The term "alloy" used in this context does not necessarily refer to the composition for bulk alloy formation, but rather, refers to two elements in the metallic state which are in intimate contact with each other. Such metal composites are sometimes referred to as bimetallic clusters and we do not differentiate the terms alloy and bimetallic cluster in this paper.

Mössbauer spectroscopy has been used to study alloy formation and the state of tin in Pt–Sn/γ-Al_2O_3 bimetallic catalysts (1–5). It was concluded that part of the tin was alloyed with platinum (1–3) and that the remainder was found as ionic Sn(II) and/or Sn(IV) species (1–5). X-ray diffraction and electron microdiffraction studies (6–8) showed that although Pt–Sn alloy was formed, most of the platinum was present as metallic platinum. Tin in excess of that needed to form the Pt–Sn alloy was not detected by energy-dispersive X-ray spectroscopy and powder X-ray diffraction. Völter *et al.* (9–13) characterized the Pt–Sn/γ-Al_2O_3 bimetallic catalysts by TPR and chemisorption techniques and used their catalysts to study reforming reactions. They found that the majority of the tin, initially present as Sn(IV), was reduced to the Sn(II) state with only 10 to 30% being reduced to Sn(0) and alloyed with the platinum.

The role of the bimetallic catalysts in controlling metal–support interaction, metal alloying and dispersion, and their subsequent effects on selectivity and lifetime in catalytic reforming can be interpreted in terms of either their electronic properties or an ensemble effect (14). It is generally agreed that in the interaction between platinum and tin the electron donation occurs from the tin to platinum (14, 15). As a result this will weaken the Pt–C bond strength during reforming reactions leading to changes in selectivity and reduced coke formation on platinum. The ensemble theory assumed that some reactions such as dehydrogenation can proceed at a single platinum atom but other reactions like hydrogenolysis require at least two to three contiguous platinum atoms (14, 16). The tin-diluted platinum surface would therefore inhibit hydrogenolysis and enhance dehydrogenation. It is also believed that the formation of a carbonaceous overlayer requires large platinum ensembles, and hence the tin-diluted platinum surface could dramatically decrease the coke formation on the metal sites and increase the lifetime of the catalyst (17, 18).

Coq and Figueras (14) and Coq *et al.* (19) identified the main role of tin as being to dilute the platinum surface since the addition of tin decreased the rate of hydrogenolysis as was the case for coke or sulfur deposition in catalytic reforming. Beltramini and Trimm (20) studied reforming reactions on mono- and bimetallic reforming catalysts. They found that less coke was formed on the bimetallic catalysts. However, the main benefit of the bimetallic catalysts originated from control of coke deposition on the active sites that give high selectivity to cycloalkanes

[1] To whom correspondence should be addressed.

0021-9517/96 $18.00

and aromatics in reforming reactions. This change in properties was interpreted as being due to either electronic modification of platinum by the tin or dilution of the platinum surface into small ensembles by the tin.

Schwank *et al.* (21–25) concluded that the electronic interaction between ionic tin and elemental platinum is the main contributor to the beneficial effects of the bimetallic catalysts, since tin was always located in close proximity to the platinum particles and the few Pt–Sn alloy particles observed did not play a significant role in controlling the catalytic behavior. XPS studies by Sexton *et al.* led to the same conclusion (26). The presence of the ionic tin–support interaction was further confirmed by Adkins and Davis (27) who used XPS to study the Pt–Sn/γ-Al_2O_3 catalysts and concluded that tin was present as an eggshell of "tin aluminate" surrounding the alumina support and the platinum was supported on this tin aluminate. This view was endorsed by Burch (15) and Burch and Garla (28) who found that tin in Pt–Sn/γ-Al_2O_3 catalysts was stabilized in the Sn(II) state by the interaction with the alumina support. The tin modified the electronic properties of the small platinum particles but no Pt–Sn alloy particles were formed, although the possibility of a solid solution of a few percentage metallic tin with platinum was not ruled out.

Transmission electron microscopy (TEM) and microanalysis by energy-dispersive X-ray spectroscopy (EDX) have proved to be powerful techniques for the study of highly dispersed bimetallic systems (29–33), giving detail of particle morphology (TEM) and the composition of small particles (EDX). In this work we report a study of Pt–Sn/γ-Al_2O_3 reforming catalysts using a parallel combination of TEM and EDX.

EXPERIMENTAL

1. Catalysts

Supported bimetallic Pt/Sn catalysts were prepared with loadings of platinum and tin varying from 0.3 to 3.0 wt% and a constant Pt/Sn weight ratio of unity. Commercial pelletized γ-Al_2O_3 (CK300, BET area 200 m^2/g) consisting of cylindrical pellets about 2 mm in diameter and ranging from 2 to 10 mm in length was used as a support. Both the bimetallic and supported Sn catalysts were prepared by a number of impregnation routes which are detailed below. The impregnated and dried materials are referred to as the catalyst precursors. All the catalysts were activated by a calcination and reduction treatment which is detailed after a description of the preparation of the precursors.

a. Pt/Sn catalysts prepared by successive impregnation with platinum and tin salts. γ-Al_2O_3 pellets were impregnated with the required concentration of H_2PtCl_6 in dilute HCl, dried for 4 h at 383 K in flowing air, and then impregnated with $SnCl_2 \cdot 2H_2O$ (aqueous) before drying at 383 K in flowing air again. The color of the pellets and the solution changed from colorless to red during the second impregnation. This change in color has been reported previously (34, 35) and has been attributed to the formation of the complex $[Pt(SnCl_3)_2\ Cl_2]^{2-}$. Catalysts prepared by this route include 0.3 wt% Pt–0.3 wt% Sn/γ-Al_2O_3 and 3.0 wt% Pt–3.0 wt% Sn/γ-Al_2O_3. The calcined and reduced precursors are referred to as 0.3 Pt–0.3 Sn (Pt first) and 3.0 Pt–3.0 Sn catalysts, respectively, in this paper.

b. Pt/Sn catalysts prepared by successive impregnation with tin and platinum salts. The preparation procedures were the same as those in (a) except that the first impregnation was carried out using $SnCl_2 \cdot 2H_2O$ in dilute HCl and the second using H_2PtCl_6. No color change was observed for samples prepared by this route. Catalysts prepared by this route include 0.3 wt% Pt–0.3 wt% Sn/γ-Al_2O_3 and 1.0 wt% Pt–1.0 wt% Sn/γ-Al_2O_3. The calcined and reduced precursors will be referred to as 0.3 Pt–0.3 Sn (Sn first) and 1.0 Pt–1.0 Sn catalysts, respectively.

c. Pt/Sn catalyst prepared by successive impregnation with tin and platinum salts in methanol. The preparation procedure was the same as that used in (b) except that the aqueous solution was replaced by methanol solution. The calcined and reduced precursor is referred to as the 0.3 Pt–0.3 Sn (methanol) catalyst.

d. Patent catalyst. This catalyst was prepared following a patient method (36). Briefly, the method involved preparing alumina gel using appropriate amounts of aluminum powder, $SnCl_2 \cdot 2H_2O$, and dilute HCl. The tin-containing alumina gel was condensed and aged in oil, then dried at 473 K and calcined at 898 K in flowing air. It was then impregnated with H_2PtCl_6 aqueous solution then dried and calcined in hydrogen at 803 K for 2 h. This catalyst is referred to as 0.3 Pt–0.3 Sn (patent). The tin in this catalyst was expected to be uniformly distributed on the alumina support, possibly forming tin aluminate.

e. Pt/Sn catalyst prepared by coimpregnation. Pellets of γ-Al_2O_3 were coimpregnated with appropriate amounts of $SnCl_2 \cdot 2H_2O$ and H_2PtCl_6 in dilute HCl and then dried in flowing air at 383 K. No color change was observed during the process. The calcined and reduced precursor is referred to as the 0.3 Pt–0.3 Sn (coimpreg.) catalyst.

f. Sn catalysts. Sn/γ-Al_2O_3 (0.3 wt%) and Sn/γ-Al_2O_3 (3.0 wt%) catalysts were prepared by impregnating the alumina support with appropriate amounts of $SnCl_2 \cdot 2H_2O$ (aqueous) and drying them in flowing air at 383 K. The calcined and reduced precursors are referred to as 0.3 Sn and 3.0 Sn catalysts, respectively.

EUROPT-3 (0.3 wt% Pt/γ-Al_2O_3, 0.95 wt% Cl) was used as a reference for comparison.

All the catalyst precursors were subjected to the following activation process:

(i) Calcination: The catalyst precursors were heated from room temperature to 673 K at 5 K/min in flowing air (60 cm^3/min) and held at this temperature for 4 h and then cooled to room temperature.

(ii) Flushing: He (60 cm^3/min) was passed over the calcined catalyst precursors for 1 h at room temperature.

(iii) Reduction: The reduction was carried out in flowing H_2 (60 cm^3/min), with a programmed temperature increase of 5 K/min from room temperature to 673 K and maintained at this temperature for 2 h. The catalysts were then cooled to room temperature in flowing hydrogen.

Further reoxidation, flushing, and reduction procedures were repeated for the above-treated specimens to investigate any further changes in the catalysts. Finally, passivation was carried out with 1.0 vol% air/He for specimens for normal TEM investigation.

2. *Catalyst Testing*

Octane reforming was carried out in a microreactor which will be described elsewhere (37) in which the reaction conditions were as follows: the H_2/octane ratio was 6/1; the reaction temperature was 783 K; the reaction pressure was 110 psig, and the weight hourly space velocity (WHSV) was 2 hr^{-1}. Analysis of the reaction products was carried out by sampling to a Shimadzu gas chromatograph.

3. *Carbon Monoxide and Oxygen Chemisorption*

Each catalyst precursor was calcined in flowing air at 673 K for 4 h prior to the chemisorption studies.

CO chemisorption was performed in a system similar to that described in an earlier publication (38). Each catalyst was heated from room temperature to 673 K in flowing hydrogen and held at this temperature for 2 h. The catalyst was then cooled to room temperature in flowing helium and the adsorption experiment was carried out by injecting pulses of known amounts of CO (4.7 cm^3, 17 Torr) into the helium carrier-gas stream and hence on to the catalyst. These injections were repeated until no further CO was adsorbed. The amount of CO adsorbed in each pulse was determined by subtracting the observed number of moles of CO that had not been retained by the catalyst from the inlet CO concentration. The total amount of CO adsorbed was the summation of these values. A similar procedure was used for oxygen chemisorption studies, pulses of oxygen being injected into helium and hence on to the reduced catalyst until no more oxygen was adsorbed.

4. *Electron Microscopy and EDX*

The microscope used was an ABT-EM002B instrument in which an EDX system LINK2000-QX with a windowless detector was installed. The microscope was usually operated at 200 kV but sometimes 160 kV was used to obtain a higher contrast image of small particles. An improved LaB_6 filament was used. The energy resolution of the EDX system was 138 eV at 5.9 keV.

Three separate TEM specimens were prepared for each dried, calcined, reduced, reoxidized, or reactor-discharged sample studied. Low magnification scans were taken of each of these to determine sample homogeneity. Many areas (>50) were examined for each TEM specimen to ensure that the reported results were truly representative of the samples. TEM specimens were prepared by putting a drop of ethanol solution containing the ground catalyst powder in suspension on a carbon film-coated copper grid. Some specimens were kept in the microscope overnight before study to minimize possible contamination during EDX spectrum collection. A beam of 10 nm in diameter, which covered a small particle, was used to generate an EDX spectrum. The collection time was usually 100 s. During the collection, the beam was sometimes spread (underfocused or overfocused) for a while to obtain an image of the particle and the beam relocated on the particle to compensate for any specimen shift. The sensitivity of the EDX system is 400–800 platinum atoms, or 2–2.5 nm particle size. The electron beam was spread to cover the whole particle when analyzing particles larger than 10 nm by EDX.

For quantitative EDX analysis, generally,

$$C_\alpha/C_\beta = K_\alpha/K_\beta \times I_\alpha/I_\beta,$$

where $C_\alpha(C_\beta)$ is the weight percent of the α (β) element, $K_\alpha(K_\beta)$ is the elemental sensitivity factor of α (β), and $I_\alpha(I_\beta)$ is the EDX intensity of α (β).

The elemental sensitivity factors K_α were taken from the operator's manual of the LINK system. They are: $K_{SnL} = 1.682$ and $K_{PtL} = 2.398$. Atomic percentage ratio of the two elements α and β is $A_\alpha/A_\beta = (C_\alpha/C_\beta) \times$ (at.wt of β/at.wt of α), i.e., atomic percent ratio of platinum to tin

$$\begin{aligned} \mathrm{Pt/Sn} &= (2.398/1.682) \times (118.7/195.1) \times (I_{Pt}/I_{Sn}) \\ &= 0.87 \times (I_{Pt}/I_{Sn}) \end{aligned}$$

Microbeam diffraction (MBD) patterns were obtained using an electron beam of 6–10 nm in diameter. For the analysis of a particle larger than 15 nm in diameter, the MBD pattern and the corresponding EDX spectrum were generated from part of the particle. MBD patterns for platinum, the elemental identity of which was verified by EDX analysis, were used as *in situ* standards for calibration of the camera length. The observed MBD patterns were compared with the patterns calculated using the lattice constants for various crystalline phases as shown in Table 1. The match between the observed MBD patterns and the calculated patterns and the EDX results were used to identify the phases present in the bimetallic particles.

5. *Ex Situ TEM and EDX*

Although catalysts were generally passivated after reduction before examination in the microscope, some *ex situ*

TABLE 1

Crystallographic Information of the Pt–Sn Crystal Systems

Formula	Crystal structure	Lattice constant (Å)			Space group
		a	*b*	*c*	
Pt	fcc	3.9231			
Pt_3Sn	fcc (Cu_3Au type)	4.0005			
PtSn	hcp (NiAs type)	4.100		5.432	$P6_3/mmc$
Pt_2Sn_3	hcp	4.337		12.960	$P6_3/mmc$
$PtSn_2$	fcc (CaF_2 type)	6.425			$Fm3m$
$PtSn_4$	Orthorhombic	6.362	6.393	11.311	C_{2v}

studies in which the catalysts were transferred after activation or reforming directly from microreactors to a dry-box filled with nitrogen without exposing them to air were also carried out. The oxygen concentration in the dry-box was less than 10 ppm. TEM samples were prepared in the drybox and then mounted on an environmental specimen holder. The environmental specimen holder enabled the TEM sample to be transferred into the microscope without exposing the sample to air.

RESULTS

1. Carbon Monoxide and Oxygen Chemisorption

The chemisorption results are presented as number of molecules of carbon monoxide or diatomic oxygen adsorbed per platinum atom for each catalyst (Table 2). Metallic platinum adsorbs both oxygen and carbon monoxide whereas metallic tin adsorbs oxygen only (39). A combination of CO and oxygen chemisorption studies should therefore give a measure of both platinum and tin dispersion provided that the adsorption stoichiometry is not altered in the presence of the second element. Carbon monoxide is known to adsorb on the platinum surface in both bridged and linear form with the latter predominating (40). The ratio of chemisorbed CO to total number of platinum atoms, i.e., CO/Pt_{total}, was found to be 0.64 for EUROPT-3 in accordance with previous studies of this catalyst (38). The $CO/Pt_{surface}$ ratio has been found to be dependent on platinum particle size (41) and values of 0.87 $\pm$ 0.07 (41, 42), 0.77 (43), 0.76 (44), and 0.75 (45, 46) have been reported. This would give a dispersion of platinum for EUROPT-3 of 74 to 84% depending on which value was adopted.

The CO/Pt_{total} values for all the 0.3 Pt–0.3 Sn catalysts were about 0.4 to 0.5 (Table 2), indicating that these catalysts were also well dispersed and that the order of impregnation with Pt and tin salts had little effect on the dispersion. CO chemisorption studies showed that the dispersion was similar for the 1.0 Pt–1.0 Sn catalyst but much poorer in the case of the 3.0 Pt–3.0 Sn catalyst.

TABLE 2

CO and O_2 Chemisorption Results for Pt–Sn/γ-Al_2O_3 Catalysts

Catalyst	Adsorbate *A*	Number of molecules per gram catalyst ($\times 10^{18}$)	A/Pt_{total}	$Sn_{total}^{Sn^0}$ [a]
0.3 Pt	CO	5.93	0.64	
EUROPT-3	O_2	4.63	1.0	
0.3 Sn	CO	0		
	O_2	0		
3.0 Sn	CO	0		
	O_2	0		
0.3 Pt–0.3Sn	CO	4.07	0.44	
Sn first	O_2	5.69	1.23	0.33
0.3 Pt–0.3 Sn	CO	3.80	0.41	
Pt first	O_2	4.49	0.97	0.20
0.3 Pt–0.3 Sn	CO	3.35	0.37	
patent	O_2	5.69	1.23	0.30
0.3 Pt–0.3 Sn	CO	4.07	0.44	
coimpreg.	O_2	4.82	1.04	0.22
0.3 Pt–0.3 Sn	CO	3.33	0.36	
methanol	O_2	4.12	0.89	0.20
1.0 Pt–1.0 Sn	CO	13.27	0.43	
Sn first	O_2	17.43	1.13	0.28
3.0 Pt–3.0 Sn	CO	9.3	0.10	
Pt first	O_2	18.1	0.39	0.14

[a] Calculated assuming that the surface stoichiometry CO/Pt = 0.76/1. O/Pt = 1/1, and O/Sn = 1/1.

The ratio of chemisorbed oxygen to total platinum, O/Pt_{total}, was found to be 1.0 for EUROPT-3 under our experimental conditions. $O/Pt_{surface}$ stoichiometries ranging from 0.5 (40, 47) to 1.0 (45, 46) have been reported in the literature, the exact stoichiometry being dependent on the exposed crystal planes (48). This suggests that EUROPT-3 has a dispersion of 100%, but CO chemisorption results have shown that a maximum of 84% of the platinum atoms are surface atoms. However, platinum is known to retain hydrogen (40). It is likely that some of the hydrogen adsorbed by the catalysts during reduction may have been retained on cooling down to room temperature prior to the chemisorption experiments. The hydrogen would be displaced by the adsorbate in the case of CO chemisorption (40), but would react with oxygen to form H_2O during the oxygen chemisorption experiment, resulting in additional oxygen being consumed. This cast some doubt on the oxygen chemisorption results for the Pt/Sn catalysts, but some qualitative conclusions can be drawn. Both 0.3 Sn and 3.0 Sn catalysts did not adsorb oxygen at all at room temperature under our experimental conditions, in agreement with previous investigations (11). This suggests that no metallic tin was formed in the Sn/γ-Al_2O_3 catalysts after reduction at 673 K. Unsupported tin oxide can be reduced to metallic tin in hydrogen at 673 K (9). It is likely therefore that the tin oxide in our catalysts was stabilized by the alumina support, possibly by the formation of a surface Sn(II)-alumina complex.

The oxygen adsorption for some Pt/Sn catalysts was found to be higher than that for the monometallic platinum catalysts even though the CO chemisorption studies had shown that the platinum dispersion was poorer in all the Pt/Sn catalysts. Indeed, the number of adsorbed oxygen atoms was found to be greater than the total number of platinum atoms for the catalysts 0.3 Pt–0.3 Sn (Sn first), 0.3 Pt–0.3 Sn (patent), 0.3 Pt–0.3 Sn (coimpreg.), and 1.0 Pt–1.0 Sn (Sn first). The excess adsorption of oxygen was used to estimate the amount of metallic tin in the bimetallic catalysts. Two assumptions were made: (i) The ratios of adsorbed CO and absorbed oxygen to platinum were not changed by tin and (ii) tin adsorbs oxygen as SnO (49). The results indicate that 20 to 33% of the tin in the 0.3 Pt–0.3 Sn and 1.0 Pt–1.0 Sn and 14% of the tin in the 3.0 Pt–3.0 Sn catalysts was reduced to the metallic state after reduction in hydrogen at 673 K, the remainder being retained as oxide. However, enrichment of tin on the surface of Pt–Sn alloys after reduction has been previously reported (50) and may also occur here, resulting in an overestimate of the amount of Sn(0) in the catalyst. This is further complicated by the fact that the adsorption stoichiometry for $CO/Pt_{surface}$ and $O/Pt_{surface}$ may change after alloy formation due to changes in particle size. Nevertheless, it would appear that only a minor part of the tin was alloyed with platinum after calcination and reduction and the fraction of the tin that is reduced to Sn(0) increased with the platinum dispersion.

2. Octane Reforming

The conversion of octane and the selectivity to aromatics for each of the Pt/Sn catalysts and EUROPT-3 are given in Table 3. The activity and selectivity of each bimetallic catalyst was found to be dependent on the way in which the catalyst had been prepared. The results in Table 3 show that catalysts prepared by either impregnating the alumina with tin before platinum or coimpregnating the alumina with tin and platinum gave higher selectivity to aromatics and overall conversion of octane than catalysts prepared by impregnating alumina with platinum before the tin. The activity of the 3.0 Pt–3.0 Sn catalyst was initially very low (2–3%) and the catalyst became inactive after 20 h on stream. A more detailed analysis of the results will be published separately (37).

In general, however, the steady-state selectivities to cracking and hydrogenolysis products were similar to that for EUROPT-3 for all the Pt/Sn catalysts, with the exception of the catalyst 0.3 Pt–0.3 Sn (methanol), which gave a slightly lower yield of cracking products and the catalyst 3.0 Pt–3.0 Sn (Pt first) where the activity rapidly declined with time. Only the 0.3 Pt–0.3 Sn (Sn first) and 0.3 Pt–0.3 Sn (coimpreg.) catalysts had higher selectivities for isomerization products than EUROPT-3 and this is in accordance with the observed high selectivity of these catalysts for aromatics.

TABLE 3

Microreactor *n*-Octane Reforming Experiments for Pt–Sn/γ-Al_2O_3 Catalysts

Catalyst	Time on stream (h)	Selectivity to aromatics (%)		Conversion of octane (%)	
		Initial	Steady	Initial	Steady
EUROPT-3 (0.3 pt)	55	35.2	41.8	48.4	27.3
0.3 Pt–0.3 Sn (Sn first)	51	28.3	54.8	51.5	38.8
0.3 Pt–0.3 Sn (Pt first)	45	36.4	39.9	45.3	32.4
0.3 Pt–0.3 Sn (patent)	45	41.3	41.8	33.1	15.1
0.3 Pt–0.3 Sn (coimpreg.)	43	53.9	54.8	61.2	35.8
0.3 Pt–0.3 Sn (methanol)	46.5	25.8	45.3	39.1	30.5
1.0 Pt–1.0 Sn (Sn first)	45.5	24.1	45.2	37.2	45.3
3.0 Pt–3.0 Sn (Pt first)	20.5				

3. TEM and EDX

a. General Observations

A summary of the TEM and EDX results is given in Table 4, where x indicates that no particle was observed in the sample. The approximate particle sizes are also presented. General features for all the catalysts are that most of the small particles (<5 nm) were platinum while most of the large particles (>10 nm) were bimetallic Pt–Sn.

As we have reported for another reforming catalyst EUROPT-4 (38), the appearance of the alumina crystallites was the same for all the catalysts studied. The alumina crystals were randomly orientated in different directions and show a range of contrast between the differently oriented crystals. A typical image of the 0.3 Pt–0.3 Sn (Sn first) catalyst after reoxidation is shown in Fig. 1a. EDX results (Fig. 1b) showed that the particle (indicated in Fig. 1 by a black arrow) was platinum. The contrast of the particle was high and the particle border sharp. Most of the small metal particles appeared to be spherical. The orientational contrast between alumina crystallites (indicated in Fig. 1 by a white arrow) was not so high and decreased continuously. However, when the difference in atomic numbers between the supported metal and aluminium was small, or neighboring alumina crystallites were at different heights in the microscope, it was difficult to distinguish orientational contrast from the contrast of metal particles supported on alumina (51). Elemental analysis was therefore used in these cases to determine if a contrast was generated by the higher atomic number of the metal, rather than orientation effects in the alumina.

b. Catalysts after Calcination and Reduction

i. 0.3 Pt–0.3 Sn catalysts. Qualitatively, the TEM results for all of the 0.3 Pt–0.3 Sn catalysts except the 0.3 Pt–0.3 Sn (methanol) catalyst were similar to each other. Only a few metallic particles were observed after calcination and

TABLE 4

Summary of TEM and EDX Results of Pt–Sn/γ-Al_2O_3 Catalyst (*x* Indicates That No Particles Were Observed in the Sample)

	0.3 Pt–0.3 Sn patent	0.3 Pt–0.3 Sn Sn first	0.3 Pt–0.3 Sn Pt first	0.3 Pt–0.3 Sn Coimpreg.	0.3 Pt–0.3 Sn methanol	1 Pt–1 Sn Sn first	3 Pt–3 Sn Pt first
1. Dried	x	x				x	x
2. Calcined	x	x	x	x	x	x	5–10 nm Pt
3. Reduced	x	Few Pt	Few Pt, few Pt–Sn	x	~2–5 nm, most Pt, few Pt–Sn	Few Pt–Sn, few Pt	<20 nm Pt Pt–Sn
4. Reoxidized	x	Few Pt	~2–5 nm, few Pt	Few Pt	~2–4 nm Pt, Pt–Sn	Few Pt, few Pt–Sn	<20 nm, most Pt, few Pt–Sn
5. Reduced	x	~2–3 nm, few Pt	~2–4 nm, few Pt	Few Pt	~2–4 nm Pt	~2–5 nm, few Pt a few Pt–Sn	<20 nm, most Pt–Sn, minor Pt–Sn
6. Reoxidized						<5 nm, most Pt, minor Pt–Sn	<10 nm, most Pt, minor Pt–Sn
7. Reduced							~5–10 nm, most Pt–Sn, minor Pt
8. After reforming	<3 nm, few Pt	<15 nm, a few Pt–Sn, minor Pt	<20 nm, a few Pt–Sn, minor Pt	<20 nm, a few Pt–Sn, minor Pt	<20 nm, a few Pt–Sn, minor Pt	<80 nm, a lot Pt–Sn, minor Pt	<100 nm, a lot Pt–Sn, minor Pt

reduction. A micrograph (Fig. 1a) and the corresponding EDX spectrum (Fig. 1b) show a particle on the alumina support for the 0.3 Pt–0.3 Sn (Sn first) catalyst after being reoxidized. The EDX spectrum was generated by an electron probe centered on the particle, the diameter of the probe being approximately equal to the distance between the two arrows in Fig. 1a. The Al and O come from the alumina support, C from the carbon film, and Cu from the copper grids. The position of Cl, Sn$L\alpha$ and Sn$L\beta$ are also indicated.

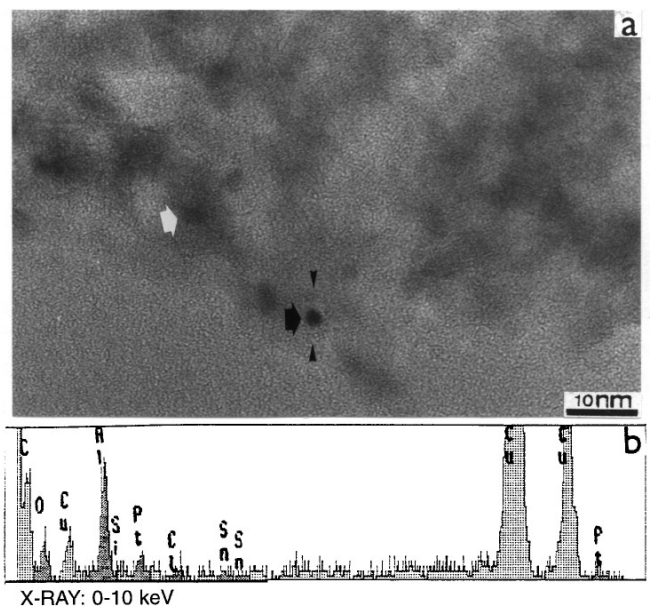

FIG. 1. 0.3 wt% Pt–0.3 wt% Sn/γ-Al_2O_3 (Sn first) catalyst after reoxidation: (a) TEM micrograph; (b) EDX spectrum from the particle and the surrounding area indicated by arrows in the figure.

No platinum or tin particles were ever observed for the 0.3 Pt–0.3 Sn (patent) catalyst before it was used in octane reforming. Although it was not possible to observe supported platinum particles smaller than 1 nm in diameter using the microscope, it is not unreasonable to suppose that there were some very small platinum particles (<1 nm) supported on the surface of the alumina. Indeed, EDX signals due to platinum and tin were obtained over a large thick area of the specimen where no particles could be seen using the microscope. Such small platinum particles have been observed in Pt–Re/γ-Al_2O_3 reforming catalyst (38). A general survey of TEM investigations over a number of areas showed that particle number densities (number of TEM-visible metal particles per unit area) were quite small for most of the 0.3 Pt–0.3 Sn catalysts, indicating that both the platinum and the tin/tin oxide in all of the four catalysts, 0.3 Pt–0.3 Sn (Sn first), 0.3 Pt–0.3 Sn (Pt first), 0.3 Pt–0.3 Sn (patent), and 0.3 Pt–0.3 Sn (coimpreg.), were well dispersed.This is in agreement with the CO chemisorption investigations. However, the particle number density for the 0.3 Pt–0.3 Sn (methanol) catalyst was higher. The particle sizes observed by TEM were also larger. A micrograph and the corresponding EXD results from a particle and the surrounding area are shown in Figs. 2a and 2b, respectively.

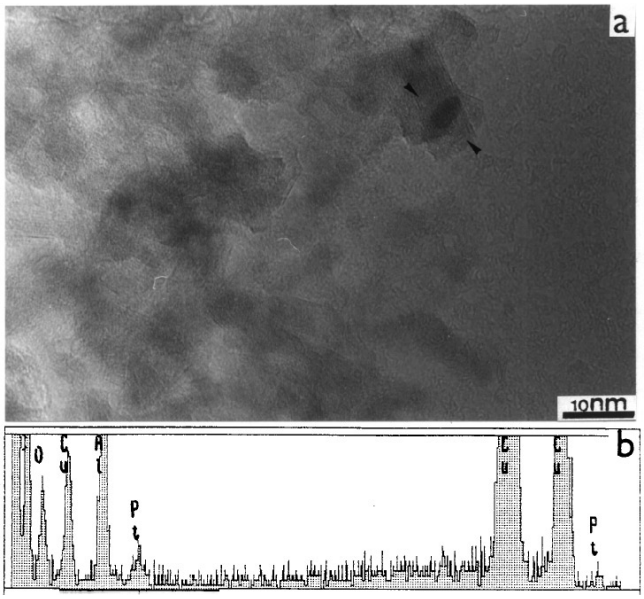

FIG. 2. 0.3 wt% Pt–0.3 wt% Sn/γ-Al_2O_3 (methanol) catalyst after calcination and reduction: (a) TEM micrograph; (b) EDX spectrum from the particle and the surrounding area indicated by arrows in the figure.

ii. 1.0 Pt–1.0 Sn catalyst. No particles were detected prior to reduction. Figure 3a shows a TEM micrograph of the 1.0 Pt–1.0 Sn catalyst precursor after calcination in air at 673 K. The EDX spectrum of the dark area indicated by the two arrows on the micrograph showed that although

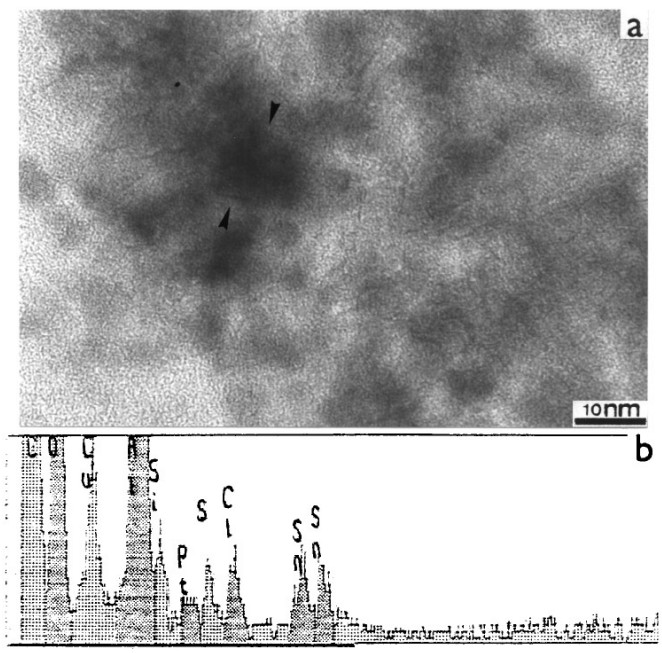

FIG. 3. 1.0 wt% Pt–1.0 wt% Sn/γ-Al_2O_3 catalyst precursor after calcination in air at 673 K: (a) TEM micrograph; (b) EDX spectrum from the dark area indicated by two arrows. The EDX results show that the elemental ratio for the dark circle is Sn/Pt = 10.

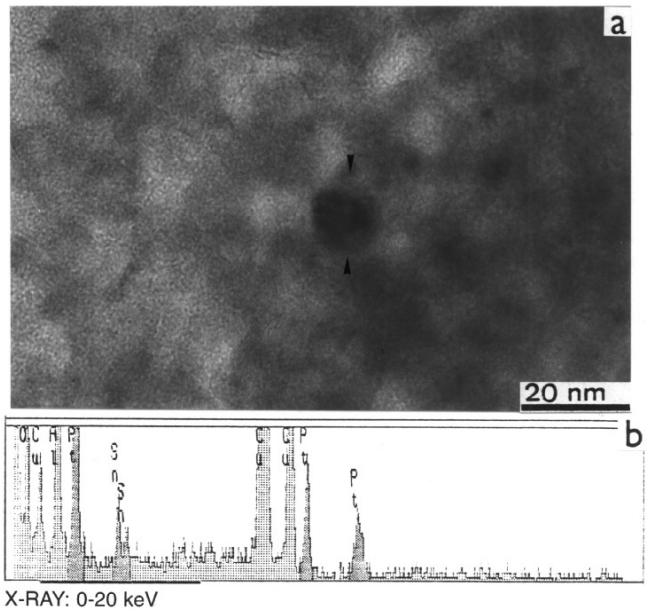

FIG. 4. 1.0 wt% Pt–1.0 wt% Sn/γ-Al_2O_3 catalyst precursor after reoxidation: (a) TEM micrograph; (b) EDX spectrum from the particle and the surrounding area indicated by arrows in the figure. Quantitative EDX results show that the elemental ratio is Pt/Sn = 1.5 for the particle.

both tin and platinum were present in the area of contrast the tin predominated. Quantitative EDX analysis revealed that the elemental ratio of Pt/Sn was about 1/10 for this area. Thus the contrast was mainly due to tin or tin oxide. The morphology of this tin or tin oxide was obviously different from that of a platinum particle which was usually circular (e.g., Fig. 1a). The gradual change of contrast across the border indicated that the tin or tin oxide interacted with the alumina support.

After reduction, some platinum and Pt–Sn alloy particles were observed in this catalyst. More metallic particles were found-after the catalyst was reoxidized and then reduced for a second time. Qualitatively, the particle number density was higher after the second reduction than that for the freshly calcined and reduced catalyst. Figure 4a shows a particle on the alumina support after reoxidation of the catalyst, and the EDX spectrum for this particle (Fig. 4b) provided evidence that the particle was a Pt–Sn alloy. Platinum particles were also observed in the reoxidized and reduced catalyst.

iii. 3.0 Pt–3.0 Sn catalyst. A survey of a number of areas of the 3% Pt/Sn catalyst showed that the average particle size and particle number density were larger than those observed for all the other catalysts studied in this work prior to their use in reforming. This made the analysis of the composition of the particles more accurate and reliable. A study of more than 100 metallic particles for the catalysts before and after reduction showed (Table 4) that most of particles in the calcined or reoxidized catalyst precursor were

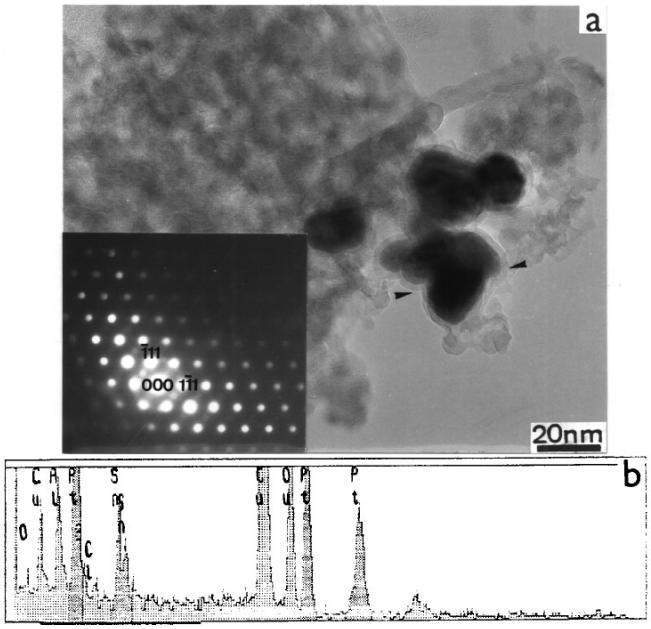

FIG. 5. 3.0 wt% Pt–3.0 wt% Sn/γ-Al_2O_3 catalyst precursor after reoxidation: (a) TEM micrograph and micro-beam diffraction for the particle indicated by arrows; (b) EDX spectrum from the particle indicated by arrows in the figure. Elemental ratio is Pt/Sn = 2.5 for the particle.

platinum while most of the particles were alloyed Pt–Sn in the reduced catalyst, and several sequential reoxidation and reduction cycles resulted in the formation of more alloy particles. Figure 5a shows a few quite large particles on the alumina support and EDX analysis (Fig. 5b) showed that one of the particles (indicated by arrows in the micrograph) had an elemental ratio of Pt/Sn = 2.5. A microbeam diffraction pattern (insert in Fig. 5a) taken from the same area used to generate the EDX spectrum (Fig. 5b) was indexed as the [110] pattern for either the face-centered cubic (fcc) platinum or the fcc Pt_3Sn structure. The fact that the stoichiometry of the particle was Pt/Sn = 2.5 and the MBD a single-phase diffraction pattern indicates that the particle was crystalline Pt_3Sn. Smaller platinum particles about 4–10 nm were also observed in this catalyst. Figure 6 shows a few platinum particles on the alumina for the 3.0 Pt–3.0 Sn catalyst after reoxidation and a second reduction.

c. Catalysts after Use in Octane Reforming

i. 0.3 Pt–0.3 Sn catalysts. There were no large differences in the TEM results for 0.3 Pt–0.3 Sn (Sn first), 0.3 Pt–0.3 Sn (Pt first), 0.3 Pt–0.3 Sn (coimpreg.), and 0.3 Pt–0.3 Sn (methanol) catalysts after use in octane reforming reactions. Particle aggregation was evident for the 0.3 Pt–0.3 Sn catalysts after use in reforming reactions. Particles were usually larger than the particles in the respective unused catalysts and most of them were Pt–Sn alloy particles.

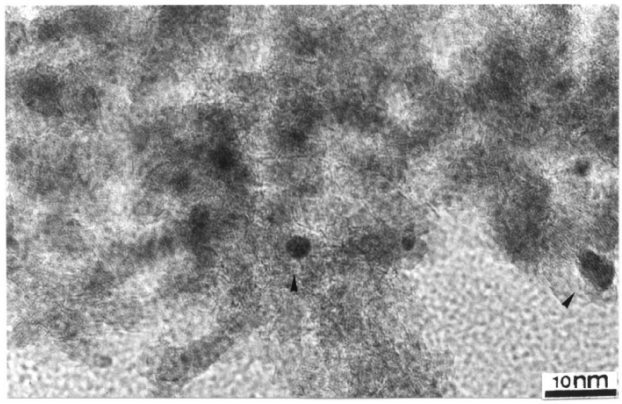

FIG. 6. TEM micrograph of 3.0 wt% Pt–3.0 wt% Sn/γ-Al_2O_3 catalyst after reoxidation and a second reduction. EDX results show that the particles indicated by the arrows are platinum.

Figure 7a shows a few particles on the alumina support for the 0.3 Pt–0.3 Sn (Sn first) catalyst after use in octane reforming. EDX analysis for one of the larger particles (indicated by arrows in the figure) proved that this was a Pt–Sn bimetallic particle. A similar micrograph for the 0.3 Pt–0.3 Sn (Pt first) catalyst after use in octane reforming is shown in Fig. 8a and the EDX (Fig. 8b) analysis for the large particle (indicated by arrows) showed that the elemental ratio was Pt/Sn = 0.87 for the particle. Figure 9a shows an image of the 0.3 Pt–0.3 Sn (coimpreg.) catalyst after use in reforming. The corresponding EDX spectrum for the particle is shown in Fig. 9b and the particle was shown to be mainly platinum with Pt/Sn = 10.

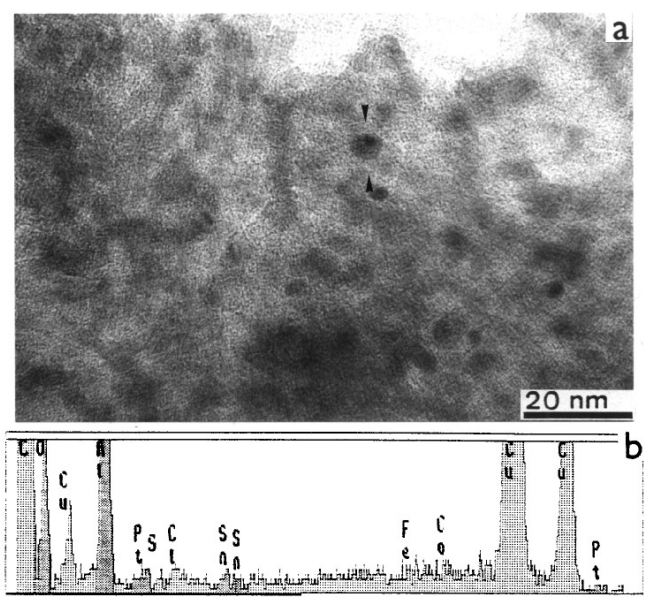

FIG. 7. 0.3 wt% Pt–0.3 wt% Sn/γ-Al_2O_3 (Sn first) catalyst after use in octane reforming: (a) TEM micrograph; (b) EDX spectrum from the particle and the surrounding area indicated by arrows.

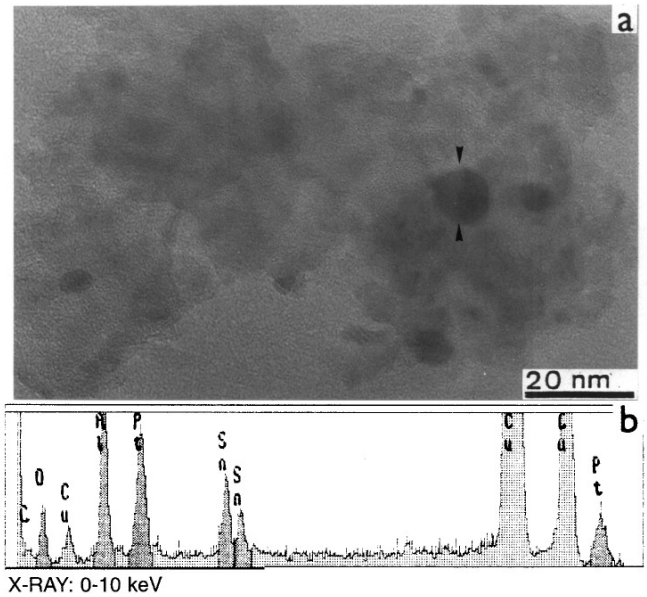

FIG. 8. 0.3 wt% Pt–0.3 wt% Sn/γ-Al_2O_3 (Pt first) catalyst after use in octane reforming: (a) TEM micrograph; (b) EDX spectrum from the particle and the surrounding area indicated by arrows. Elemental ratio in Pt/Sn = 0.87 for the particle.

Only a few small platinum particles were observed for the 0.3 Pt–0.3 Sn (patent) catalyst after use in reforming. This indicates that the high-temperature calcination treatment used in the preparation of this catalyst resulted in strong metal–support interactions between the tin and alumina, possibly also involving platinum which resisted particle aggregation during the octane reforming reactions.

ii. 1.0 Pt–1.0 Sn catalyst. Particle aggregation and further alloy formation occurred after the 1.0 Pt–1.0 Sn catalyst had been used for octane reforming. Large particles of a few tens of nanometers in diameter were found and most of them were bimetallic particles. However, the composition of the particles was found to vary from particle to particle. MBD was carried out for some particles in addition to the EDX analysis in order to identify the structural phase of the particles.

Figure 10 shows a large particle on alumina. EDX analysis showed that the particle consisted of platinum only. The inset MBD is the [110] pattern of the crystalline platinum. The distances of platinum diffraction spots 111 and 002 were used as a standard for calibration of the camera length of the MBD mode. Figure 11a shows another particle and the corresponding EDX spectrum (Fig. 11b) for the area (a part of the particle) indicated by two arrows on the micrograph. The composition of the section of the particle in the selected area was found to be Pt/Sn = 0.92 and the MBD pattern inset was indexed as the [121] pattern of the PtSn hcp structure. Therefore the existence of the PtSn alloy phase was identified in the reactor-discharged 1.0 Pt–1.0 Sn catalyst by both the EDX and MBD analysis.

Figure 12a shows a particle supported on the alumina. The MBD pattern from a selected area of the particle (indicated by two arrows) was inserted onto the micrograph and the corresponding EDX spectrum is shown in Fig. 12b. Quantitative EDX analysis showed that the stoichiometry for the area studied was Pt/Sn = 2.0. However, the diffraction pattern did not correspond to any known Pt–Sn bimetallic phases listed in Table 1. The lattice distances corresponding to diffraction spots a, b, c, and d (Fig. 12a) are at 0.228, 0.171, 0.197, and 0.137 nm, respectively. It is unlikely that these lattice distances can be assigned to the

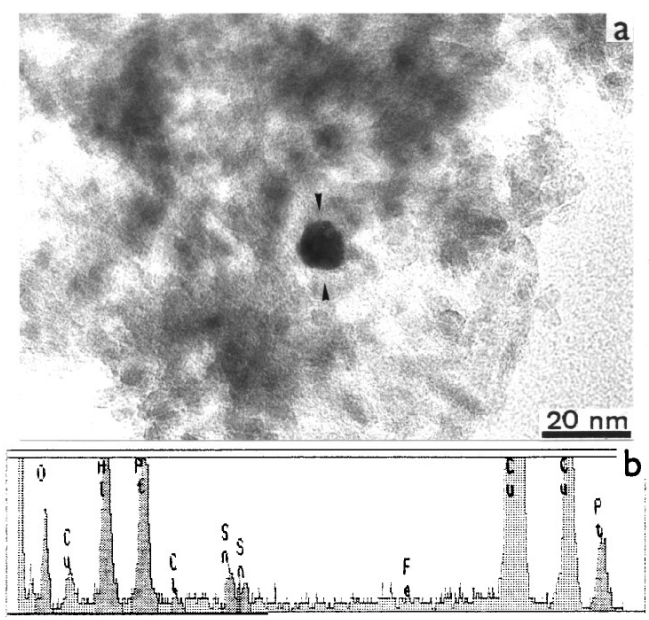

FIG. 9. 0.3 wt% Pt–0.3 wt% Sn/γ-Al_2O_3 (coimpregnated) catalyst after use in octane reforming: (a) TEM micrograph; (b) EDX spectrum from the particle and the surrounding area indicated by arrows. Elemental ratio is Pt/Sn = 10 for the particle.

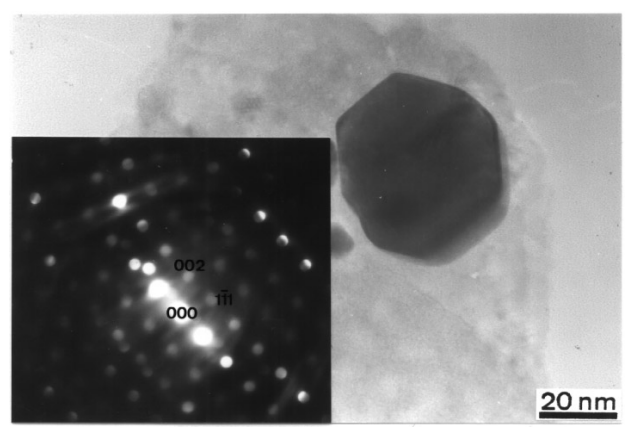

FIG. 10. TEM micrograph of 1.0 wt% Pt–1.0 wt% Sn/γ-Al_2O_3 catalyst after use in octane reforming. EDX results show that the particle is platinum. Insert [110] MBD pattern of the crystalline platinum.

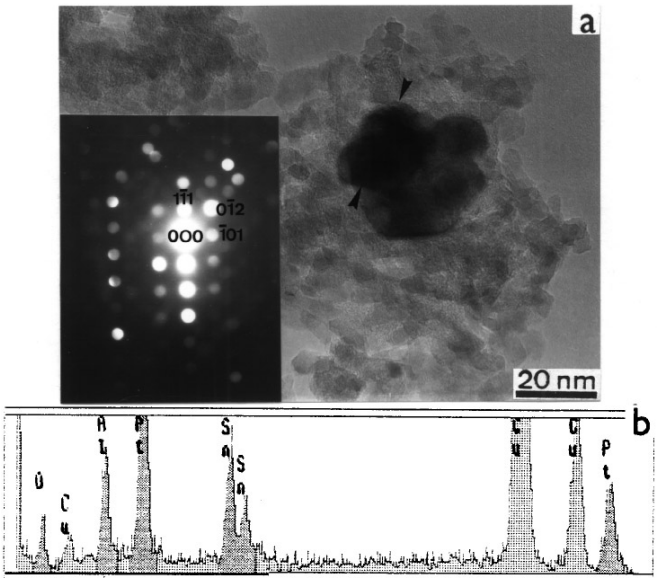

FIG. 11. 1.0 wt% Pt–1.0 wt% Sn/γ-Al_2O_3 catalyst after use in octane reforming: (a) TEM micrograph; (b) EDX spectrum from the area indicated by two arrows. The inset MBD pattern in (a) is the [121] pattern of the crystalline PtSn hcp structure. Quantitative EDX results show that the elemental ratio is Pt/Sn = 0.92 for the particle.

distorted [110] pattern of the fcc Pt_3Sn because the variation of lattice distance would then be too large (>0.03 nm). The results therefore point to the existence of another Pt–Sn bimetallic phase with stoichiometry approximately Pt_2Sn. However, further work is needed to confirm this.

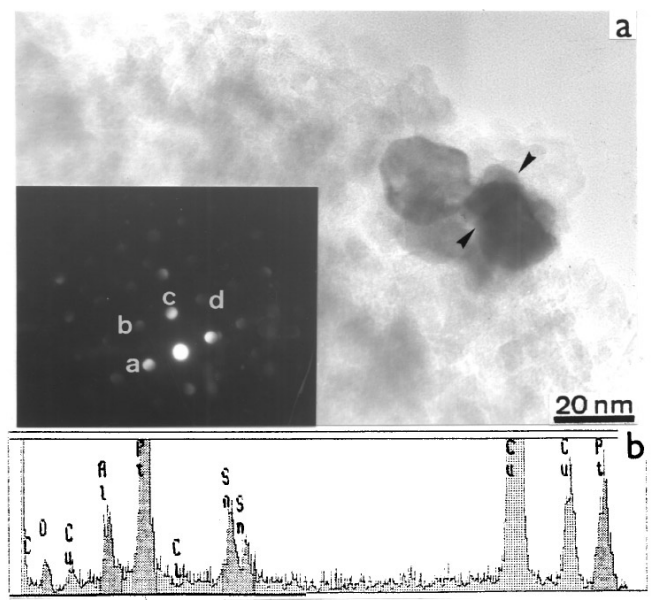

FIG. 12. 1.0 wt% Pt–1.0 wt% Sn/γ-Al_2O_3 catalyst after use in octane reforming: (a) TEM micrograph; (b) EDX spectrum from the area indicated by two arrows. Quantitative EDX results show that the elemental ratio is Pt/Sn = 2.0 for the particle.

iii. 3.0 Pt–3.0 Sn catalyst. Very large particles up to 100 nm were observed for the 3.0 Pt–3.0 Sn catalyst after use in octane reforming. Most large particles were bimetallic particles although single platinum particles were also found. EDX results showed that the elemental ratio of Pt/Sn was much greater than one for some areas but much less than one for some other areas, indicating a nonuniform distribution of the two elements in this catalyst.

d. Metal Distributions

To understand the distribution of metals in the bimetallic catalyst, further investigations were carried out by varying the probe size of the electron beam used in the EDX experiment. To do this experiment, an area of the sample was selected that contained a single large particle and a reasonably uniform thickness of alumina support around the particle. Initially, a beam about the same size (~10 nm) as the particle was used to generate a EDX spectrum, and the beam was then defocused (underfocused or overfocused) to the larger size of 100 nm to obtain another spectrum. The collection time was generally around 100 s. The dead time and counts per second were kept the same for every spectrum. When the beam is spread, the total current of the beam will remain the same, so its intensity will decrease with the square of the beam size. At the same time, the specimen material included within the beam will increase as the square of the beam diameter. This means that the EDX intensity should be a constant if one element is uniformly distributed. Further spectra were collected using 200- and 500-nm-diameter beams, respectively. The intensities of platinum and tin were then plotted as a function of the beam size (Fig. 13). For comparison, a theoretical platinum intensity curve is also included. This was derived by assuming that only the platinum particle was present on the alumina.

Figure 13 shows the intensities of platinum and tin as a function of the probe size for the 1.0 Pt–1.0 Sn cata-

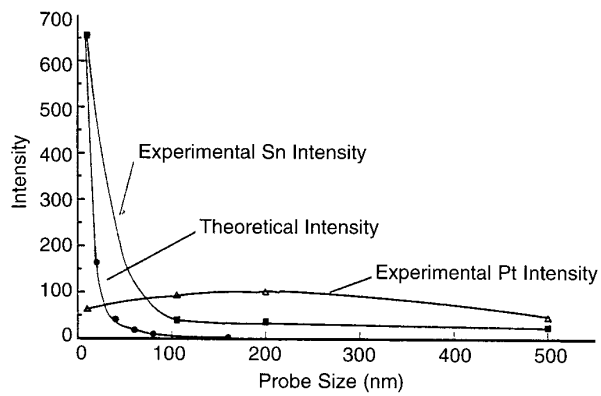

FIG. 13. The EDX intensities of platinum and tin as a function of the probe size for the 1.0 wt% Pt–1.0 wt% Sn/γ-Al_2O_3 catalyst after reoxidation and a second reduction.

lyst after being reoxidized and reduced for a second time. The platinum intensity was found to be almost constant when the beam diameter was greater than or equal to 100 nm. The theoretical intensity curve based on a single platinum particle at the center of the beam shows that the intensity should actually be zero when the beam is 100 nm or more. This indicated that a second type of platinum species was also present. This platinum species may consist of very small platinum particles which could not be resolved by the microscope when they were supported on alumina. This hypothesis is supported by our previous assumption that small (<1 nm) particles were present in the catalysts. This is also in agreement with previous work in this laboratory (52) in which quantitative X-ray diffraction, hydrogen chemisorption, and high-resolution electron microscopy studies showed that the average platinum particle size was 0.9 nm in 0.5 wt% Pt/γ-Al_2O_3 catalysts. For tin, the intensity was almost a constant. This suggests that tin or tin oxide was distributed as a TEM-invisible even layer of small particles supported on the surface of alumina. The tin intensity was higher than the platinum intensity when the beam was large enough so that the tin intensity from the electron-illuminated area representing the average concentration of tin in the catalyst was due to the fact that the two elemental sensitivity factors are different for platinum and tin. When the metal loadings are the same for platinum and tin, as in this catalyst, $I_{Pt}/I_{Sn} = K_{Sn}/K_{Pt} = 1.682/2.398 = 0.7$.

This variable beam size experiment was repeated for the 1.0 Pt–1.0 Sn catalyst after use in reforming. Figure 14a shows a particle on a reasonably uniform thickness alumina support. The particle was found to be a Pt–Sn alloy particle. The experimental EDX intensities for platinum and tin as a function of the beam diameter are shown in Fig. 14b. A theoretical EDX intensity curve is also presented. This was obtained by assuming that only the single particle was present at the center of the area. This particle would produce the same tin intensity as the experimental one when the electron probe was the same size as the particle. It was found that the experimental intensities of tin were twice as large as the theoretical intensities when the beam diameter was larger than 300 nm. The difference between the experimental and the theoretical platinum intensities was smaller. This indicated that another tin and platinum species was present. However, the difference between the experimental and the theoretical intensities was smaller than that observed for the unused catalyst. This indicated that particle sintering (or aggregation) resulted in the loss of neighboring small particles.

e. Ex Situ Studies

Ex situ studies were carried out using both calcined and reduced catalysts and catalysts after use in reforming. The TEM results for these oxygen-free prepared samples were identical to those obtained using the standard procedure of

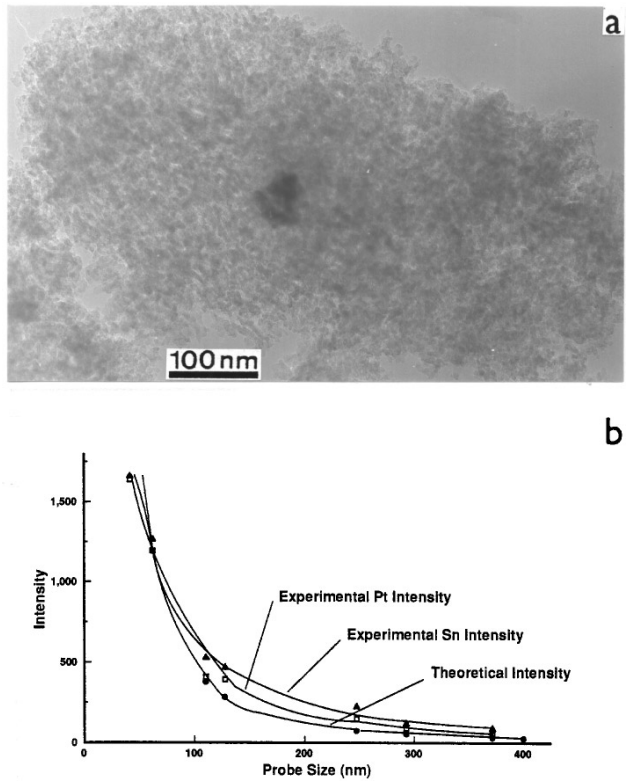

FIG. 14. 1.0 wt% Pt–1.0 wt% Sn/γ-Al_2O_3 catalyst after use in octane reforming: (a) TEM micrograph; (b) The EDX intensities of platinum and tin as a function of the probe size. The particle is an alloyed PtSn.

passivation of the reduced/reactor discharged samples in 1 vol% air/helium. Furthermore, subsequent exposure of the *ex situ* samples to air for up to 24 h did not change the particle morphology or size, indicating that the platinum and tin oxide were stable at room temperature in air. Moreover, TEM results for the catalysts which had been aged in air at room temperature for 2 months did not differ greatly from the results discussed above. Collectively, these data show that the observed results are representative of the particle morphology and size distribution of the catalysts in the reactor.

DISCUSSION

Chemisorption studies for EUROPT-3 showed that platinum was well dispersed and, indeed, no metal particles were observed by TEM prior to reforming (38). The platinum was also well dispersed in all of the 0.3 Pt–0.3 Sn bimetallic catalysts with only a few small platinum particles being observed by TEM prior to reforming. TEM and EDX studies of 0.3 Pt–0.3 Sn (Sn first), 0.3 Pt–0.3 Sn (Pt first), and 0.3 Pt–0.3 Sn (coimpreg.) catalysts after use in octane reforming showed that particle aggregation had occurred in each case to form particles up to 20 nm in size. Although some platinum particles were still detected, the majority of

the particles were bimetallic with a Pt/Sn ratio of 1/1. There was also a significant number of very small TEM-invisible (<1 nm) platinum particles in all of the catalysts. A similar particle size distribution was observed in EUROPT-3 after it had been used in octane reforming. A significant number of small Pt particles (<5 nm) were observed together with larger particles (<20 nm) in EUROPT-3 after it had been used in reforming (38).

The steady-state conversion of octane was higher for the 0.3 Pt–0.3 Sn (Sn first), 0.3 Pt–0.3 Sn (Pt first), and 0.3 Pt–0.3 Sn (coimpreg.) catalysts than for EUROPT-3, and 0.3 Pt–0.3 Sn (Sn first) and 0.3 Pt-0.3 Sn (coimpreg.) catalysts gave the highest steady-state selectivities for both aromatics and isomerized products of all the catalysts studied. The selectivity for 0.3 Pt–0.3 Sn (Pt first) was much lower. Since the dispersion, extent of alloying and composition of the alloy were similar in all three catalysts, the observed differences in selectivity may be related to differences in the modification of the small platinum particles. The modification would arise from interaction between platinum and tin or tin oxide leading to changes in he electronic properties of the platinum (25). Alternatively, the observed differences in selectivity may be due to variations in the precursor state. The 0.3 Pt–0.3 Sn (Pt first) differed from the 0.3 Pt–0.3 Sn (coimpreg.) and 0.3 Pt–0.3 Sn (Sn first) catalysts in that the complex $[Pt\,(SnCl_3)_2Cl_2]^{2-}$ was thought to be formed during the impregnation step (see Experimental section). Previous studies (53) have shown that reduced $[Pt\,(SnCl_3)Cl_2]^{2-}/\gamma$-$Al_2O_3$ is a poorer catalyst for both cyclohexane dehydrogenation and cyclopentane hydrogenolysis compared with Pt–Sn/γ-Al_2O_3 prepared by either a coimpregnation route or by successively impregnating the support with $SnCl_2$ and H_2PtCl_6 in accordance with our findings.

The 0.3 Pt–0.3 Sn (methanol) catalyst differed from the 0.3 Pt–0.3 Sn (Sn first) catalyst only in that methanol rather than water was used for impregnation of the metal salts. This had an effect on the structure of the catalyst, with a poorer platinum dispersion and more alloy formation occurring on reduction for the 0.3 Pt–0.3 Sn (methanol) catalyst. This resulted in the conversion and selectivity to aromatics being lower for the 0.3 Pt–0.3 Sn (methanol) than for the 0.3 Pt–0.3 Sn (Sn first) catalyst.

The platinum dispersion for the 1.0 Pt–1.0 Sn catalyst was comparable to that of all the 0.3 Pt–0.3 Sn catalysts, and it showed the highest steady-state conversion of octane. This may reflect the increase in the number of small TEM-visible and -invisible platinum particles in the catalyst. The steady-state selectivity to aromatics was slightly higher than that for EUROPT-3. This may have been due to electronic modification of the very small platinum particles and/or alloy formation. There was no significant variation in the yield of cracking products at the steady state for any of the 0.3 Pt–0.3 Sn and the 1.0 Pt–1.0 Sn catalysts, and they were approximately the same as that for EUROPT-3 (37), indicating that the tin was not modifying the acidity of the support.

The 3.0 Pt–3.0 Sn catalyst had a poor platinum dispersion and fairly extensive Pt–Sn alloy formation occurred on reduction. It was a very poor reforming catalyst that aggregated extensively during reaction. It is likely that the high concentration of tin poisoned the catalytically active platinum sites, as discussed previously (54).

TEM and EDX results showed that platinum and tin tend to be alloyed and Pt–Sn alloys were readily formed in the bimetallic catalysts as evidenced by the observed alloys in all of the bimetallic catalysts after either several oxidation and reduction cycles or after use in octane reforming. It is likely that both the electronically modified platinum particles and the small Pt–Sn alloy particles contributed to the improved selectivity and stability of the bimetallic reforming catalysts. Alloy formation would favor the formation of small platinum ensembles by diluting the particle surface. Reactions such as aromatization, which take place on either single platinum atom sites or small ensembles, were therefore enhanced and undesired reactions such as hydrogenolysis and coke formation that require larger ensembles were inhibited (14, 16–18). Alloy formation may also lead to platinum redispersion during the reactivation process. Evidence for this is provided by the observation that the 1.0 Pt–1.0 Sn and 3.0 Pt–3.0 Sn catalysts were composed mainly of Pt–Sn alloy particles after reduction but the majority of the particles were platinum after reoxidation.

It would therefore appear that the increased selectivity of the Pt–Sn/ γ-Al_2O_3 catalysts compared to Pt/γ-Al_2O_3 results from the complex interplay between the electronically modified platinum by tin/tin oxide and the formation of Pt–Sn alloys. The overall conversion was governed by the number of surface platinum atoms.

CONCLUSIONS

(1) The Pt–Sn/γ-Al_2O catalysts contained a significant number of TEM-invisible platinum particles less than 1 nm in diameter in addition to larger TEM-visible particles.

(2) The majority of the tin was found in the ionic Sn(II) state for the catalyst after reduction at 673 K. However, a small amount of the tin was reduced to the metallic state after reduction at 673 K in hydrogen in the presence of platinum, and Pt–Sn alloys were formed in the bimetallic catalysts. The extent of alloy formation increased with increasing metal loadings. Most of the alloy particles were PtSn. Pt–Sn clusters with other stoichiometries as well as platinum particles were also observed for the bimetallic catalysts.

(3) More bimetallic particles were formed after several reoxidation and reduction cycles, indicating that platinum and tin tend to form alloys in the bimetallic catalysts.

(4) Particle aggregation occurred during the reforming reaction. Most of the large particles were alloy particles. The major alloy phase was PtSn. Platinum and other compositions of Pt–Sn alloys were also observed for the catalysts after octane reforming.

(5) Catalyst performance was found to be dependent on the way in which the catalyst was prepared.

ACKNOWLEDGMENTS

Financial support from the Initiative in Interfaces and Catalysis of SERC is gratefully acknowledged. Z. Huang thanks Mr. D. Thom for technical help.

REFERENCES

1. Bacaud, R., Bussière, P., and Figueras, F., *J. Catal.* **69**, 399 (1981).
2. Li, Y., Klabunde, K. J., and Davis, B. H., *J. Catal.* **128**, 1 (1991).
3. Kuznetsov, V. I., Belyi, A. S., Yurchenko, E. N., Smolikov, M. D., Protasova, M. T., Zatolokina, E. V., and Duplyakin, V. K., *J. Catal.* **99**, 159 (1986).
4. Vertes, Cs., Talas, E., Czako-Nagy, I., Ryczkowski, J., Göbölös, S., Vertes, A., and Margitfalvi, J., *Appl. Catal.* **68**, 149 (1991).
5. Hobson, M. C., Goresh, S. L., and Khare, G. P., *J. Catal.* **142**, 641 (1993).
6. Srinivasan, R., Angelis, R. J., and Davis, B. H., *J. Catal.* **106**, 449 (1987).
7. Srinivasan, R., Rice, L. A., and Davis, B. H., *J. Catal.* **129**, 257 (1991).
8. Davis, B. H., *in* "Proceedings, 10th International Congress on Catalysis, Budapest, 1992" (L Guczi, F. Solymosi, and P. Tétényi, Eds.), p. 137. Akadémiai Kiadó, Budapest, 1993.
9. Völter, J., Lietz, G., Uhlemann, M., and Hermann, M., *J. Catal.* **68**, 42 (1981).
10. Völter, J., and Kürschner, U., *Appl. Catal.* **8**, 167 (1987).
11. Lieske, H., and Völter, J., *J. Catal.* **90**, 96 (1984).
12. Palazov, A., Bonev, Ch., Shopov, D., Lietz, J., Sárkány, A., and Völter, J., *J. Catal.* **103**, 249 (1987).
13. Lieske, H., Sárkány, A., and Völter, J., *Appl. Catal.* **30**, 69 (1987).
14. Coq, B., and Figueras, F., *J. Catal.* **85**, 197 (1984).
15. Burch, R., *J. Catal.* **71**, 348 (1981).
16. Biloen, P., Dautzenberg, F. M., and Sachtler, W. M. H., *J. Catal.* **50**, 77 (1977).
17. Parera, J. M., and Beltramini, J. N., *J. Catal.* **112**, 357 (1988).
18. Barbier, J., Corro, G., Zhang, Y., Bournonville, J. P., and Franck, J. P., *Appl. Catal.* **16**, 169 (1985).
19. Coq, B., Chaqroune, A., Figueras, F., and Nciri, B., *Appl. Catal.* **82**, 231 (1992).
20. Beltramini, J., and Trimm, D. L., *Appl. Catal*. **32**, 71 (1987).
21. Schwank, J., Balakrishnan, K., and Sachdev, A., *in* "Proceedings, 10th International Congress on Catalysis, Budapest, 1992" (L. Guczi, F. Solymosi, and P. Tetenyi, Eds.), p. 140. Akadémiai Kiadó, Budapest 1993.
22. Sachdev, A., and Schwank, J., *in* "Proceedings,12th International Congress for Electron Microscopy," Vol. IV, p. 278. San Francisco Press, San Francisco, 1990.
23. Balakrishnan, K., and Schwank, J., *J. Catal.* **138**, 491 (1992).
24. Balakrishnan, K., and Schwank, J., *J. Catal.* **127**, 287 (1991).
25. Balakrishnan, K., and Schwank, J., *J. Catal.* **132**, 451 (1991).
26. Sexton, B. A., Hughes, A. E., and Foger, K., *J. Catal.* **88**, 466 (1984).
27. Adkins, S. R., and Davis, B. H. *J. Catal.* **89**, 371 (1984).
28. Burch, R., and Garla, L. C., *J. Catal.* **71**, 360 (1981).
29. Blanchard, G., Charcosset, H., Dexpert, H., Freund, E., Leclercq, C., and Martino, G., *J. Catal.* **70**, 168 (1981).
30. Sachdev, A., and Schwank, J., *J. Catal.* **120**, 353 (1989).
31. Handy, B. E., Dumesic, J. A., Sherwood, R. D., and Baker, R. T. K., *J. Catal.* **124**, 160 (1990).
32. Srinivasan, R., and Davis, B. H., *Appl. Catal. A* **87**, 45 (1992).
33. Datye, A. K., and Smith, D. J., *Catal. Rev.- Sci. Eng.* **34**, 129 (1992).
34. Bond, G. C., and Hellier, M., *J. Catal.* **7**, 217 (1967).
35. Young, J. F., Gillard, R. D., and Wilkinson, G., *J. Chem. Soc.,* 5179 (1964).
36. Antos, G. J., U.S. Patent, 3 929 683, Dec. 1975.
37. Park, C., and Webb, G., Unpublished.
38. Huang, Z., Fryer, J. R., Park, C., Stirling, D., and Webb, G., *J. Catal.* **148**, 478 (1994).
39. Bond, G. C., "Catalysis by Metals." Academic Press, London, 1962.
40. Jackson, S. D., Glanville, B. M., Willis, J., McLellan, G. D., Webb, G., Moyes, R. B., Simpson, S., Wells, P. B., and Whyman, R., *J. Catal.* **139**, 207 (1993).
41. Herz, R. K., and McCready, D. F., *J. Catal.* **81**, 358 (1983).
42. Dorling, T. A., and Moss, R. L., *J. Catal.* **7**, 378 (1967).
43. Norton, P. R., Davies, J. A., Creber, D. K., Sitter, C. W., and Jackson, T. E., *Surf. Sci*. **108**, 205 (1981).
44. Verbeek, H., and Sachtler, W. M. H., *J. Catal.* **42**, 257 (1976).
45. Gruber, H. L., *J. Phys. Chem.* **66**, 48 (1962).
46. Benson, J. E., and Boudart, M., *J. Catal.* **4**, 704 (1965).
47. Wilson, G. R., and Hall, W. K., *J. Catal.* **17**, 190 (1970).
48. Tucker, C. W., *Surf. Sci.* **2**, 516 (1964).
49. Powell, R. A., *Appl. Surf. Sci.* **2**, 397 (1979).
50. Bouwman, R., and Biloen, P., *Anal. Chem.* **46**, 136 (1974); Bouwman, R., Toneman, L. H., and Holscher, A. A., *Surf. Sci.* **35**, 8 (1973).
51. Yacaman, M., and Avalos, M., *Catal. Rev.-Sci. Eng.* **34**, 55 (1992).
52. Butterly, L. J., Baird, T., Fryer, J. R., Day, M., and Norval, S., *in* "Proceedings, 11th International Congress on Electron Microscopy" (T. Imura, S. Maruse, and T. Suzuki, Eds.), Vol. II, p. 1775. The Japanese Society of Electron Microscopy, Tokyo, 1986.
53. Miguel, S. R., Baronetti, G. T., Castro, A. A., and Scelza, O. A., *Appl. Catal.* **45**, 61 (1988).
54. Dautzenberg, F. M., Helle, J. N., Biloen, P., and Sachtler, W. M. H., *J. Catal.* **63**, 119 (1980).